Electronic Research Archive

https://www.aimspress.com/journal/era

ERA, 33(8): 4917–4932.
DOI: 10.3934/era.2025221
Received: 02 July 2025
Revised: 10 August 2025
Accepted: 18 August 2025
Published: 22 August 2025

Research article

Output feedback maneuvering control of random Lagrange systems with actuator malfunctions

Cun Yang*

School of Mathematics and Informational Science, Shandong Technology and Business University, Yantai 264005, China

* **Correspondence:** Email: yangcongcong163@163.com.

Abstract: In this paper, a fault-tolerant output feedback maneuvering control scheme with prescribed performance for a class of random Euler–Lagrange systems with unmeasurable velocity and actuator faults is presented. First, an adjustable velocity observer is ingeniously constructed without additional dynamic compensation signals. Second, a projection operator is used to estimate the actuator fault factors. Based on the designed observer and projection operator, a static controller is designed to address geometric tasks with performance constraints, while a dynamic controller is developed to achieve speed allocation tasks. Finally, the effectiveness of the proposed control method is demonstrated through an illustrative example involving a two-link robotic system operating in a random environment.

Keywords: Euler–Lagrange system; maneuvering; colored noise; loss of effectiveness fault; velocity observer

1. Introduction

In recent decades, the issue of fault control in Euler–Lagrange (EL) systems has garnered significant research attention. In engineering applications, the complexity of system structures and the prolonged operational duration often lead to malfunctions in actuators and sensors during system operation, which may cause unpredictable consequences. The basic actuator faults commonly include the following: lock-in-place, hard-over or saturation, loss of effectiveness, float, and bias, as documented in [1, 2]. To maintain the performance metrics of the closed-loop system in the presence of mechanical faults, it is crucial to develop effective fault-tolerant control (FTC) strategies. Generally speaking, some methods for handling actuator faults include sliding mode [3, 4], feedforward neural network [5, 6], fault detection observer [7, 8], and adaptive compensation [9, 10], among others. [11] investigated FTC for networked flexible robotic manipulators subject to actuator faults, input saturation, and external disturbances. In scenarios where the reference trajectory is unknown a priori and actuator failures occur, [12] proposed

a novel fault compensation scheme to address the output-constrained tracking control problem in EL systems. To reduce costs and maintain mechanical system flexibility, speed sensors are often omitted, necessitating the design of an output feedback controller. Roughly speaking, the existing results on output feedback control of EL systems are mainly categorized into two types: semi-global [13, 14] and global [15, 16]. Although the latter achieves global stability, the designed observer is complex and requires the introduction of additional dynamic variables.

Although significant contributions to FTC and output feedback design were made in the aforementioned paper, only trajectory tracking problems were addressed. In contrast to trajectory tracking, maneuverability along parameterized paths also represents an important research focus [17, 18]. The problem of maneuverability involves two objectives: the geometric objective, which ensures compliance with spatial constraints in the output space, and the dynamic objective, which satisfies the requirements for dynamic behavior along the path. The maneuvering problem enables spatiotemporal decoupling and finds applications in various domains, such as ocean surface vehicles [19, 20] and unmanned aerial vehicles [21,22]. It is worth noting that research on the maneuverability of EL systems remains relatively limited. Similar to the performance constraint issue in trajectory tracking, the convergence accuracy and transient response of EL systems must also be taken into account when executing geometric tasks. To guarantee that output errors remain within prescribed bounds for both convergence rate and maximum overshoot, performance-constrained guidance laws can be formulated using various methods, including barrier Lyapunov function [23], funnel control method [24], and error transformation [25–27].

Given that mechanical systems often operate in random vibration environments, it is crucial to investigate the maneuverability of EL systems under actuator failures and unmeasurable velocity states in stochastic conditions. In this context, [28] proposed a tracking control problem for a class of random nonlinear systems in the sense of second-order moments suffering from actuator faults. Based on a novel high-gain observer, [29] investigated the global output feedback trajectory tracking control problem of random EL systems. In contrast to [29], the maneuvering control problem of random Lagrangian systems is first addressed in this paper, under actuator faults and unmeasurable disturbances with unmeasurable velocity signals. For a class of stochastic strict feedback nonlinear systems with uncertainties, adaptive fuzzy fault-tolerant control with input quantization was researched in [30]. By combining the prescribed performance technique with the command filter, an adaptive fuzzy tracking control of a stochastic system was studied in [31]. Compared with stochastic nonlinear systems driven by white noise, random nonlinear systems offer distinct advantages in handling more generalized noise profiles, such as colored noise. Since white noise does not exist in real-world scenarios, random EL systems disturbed by colored noise are also worthy of further exploration. Building upon these observations, for random EL systems with actuator malfunctions and unmeasurable velocity, this paper proposes an output feedback FTC maneuvering controller with prescribed performances to achieve semi-global practical stability in probability of error system. The proposed scheme exhibits the following features:

1) In contrast to trajectory tracking of Lagrangian systems [4, 12, 15, 24], the maneuverability control scheme exhibits spatiotemporal decoupling characteristics by enabling the separation of geometric and dynamic objectives. By introducing appropriate error transformations, stable functions with reduced complexity can be constructed, thereby achieving performance constraints for the geometric tasks of Lagrangian systems.

2) Based on [17, 18], the maneuvering problem is combined with fault-tolerant control, output feedback, and constrained performances, and is extended to random situations. In the framework of

stochastic analysis, it is rigorously proven that all signals in a closed-loop system are probabilistically bounded by adopting the practical parameter-tuning principle.

Notations: $\mathbb{R}^n$ denotes the real n-dimensional space; $\mathbb{R}^{m\times n}$ denotes the real $m \times n$ matrix space; diag$\{\cdot\}$ transforms a vector into a diagonal matrix. For a vector x, x^T denotes its transpose, and $|x|$ indicates the Euclidean norm; for a matrix X, X^{-1} is the inverse matrix, $|X|$ signifies the Euclidean norm. Let $\lambda_{\min}(X)$ indicate the minimum eigenvalue. $B(x_0, r) = \{x \in \mathbb{R}^n : |x - x_0| \le r\}$ stands for a ball with x_0 as the center and r as the radius. $\frac{\partial y}{\partial x}$ is the derivative of a vector y to a vector or a scalar x. $I_{n\times n}$ represents the $n \times n$ unit matrix; E expresses the mathematical expectation.

2. Problem setup

Consider the EL system subject to random disturbances

$$H(q)\ddot{q} + C(q, \dot{q})\dot{q} + h(q) = -k\dot{q} + \delta u + \Phi(q)\xi, \tag{2.1}$$

where $q \in \mathbb{R}^m$ is the generalized coordinate, $H(q), C(q, \dot{q}) \in \mathbb{R}^{m\times m}$ denote the generalized mass matrix and the Coriolis matrix, respectively, $h(q) \in \mathbb{R}^m$ is potential force, k is a diagonal friction matrix, and $\delta = \text{diag}\{\delta_1, \cdots, \delta_m\}$ is the actuator efficiency matrix, where $\delta_i \in [\delta_0, 1]$ $(0 < \delta_0 < 1)$ is an unknown remaining control rate coefficient of the i-th actuator, which denotes that the corresponding actuator loses some efficiency. $u \in \mathbb{R}^m$ is the control input, $\Phi(q) \in \mathbb{R}^{m\times n}$ is the disturbance matrix, and $\xi \in \mathbb{R}^n$ represents random disturbance. In the case of $\delta = I_{m\times m}$, indicating that the EL system in a fault-free condition, then the system can be simplified to the model in [29].

For the subsequent convenience of controller design, the following familiar properties are required with respect to system (2.1).

Property 1. The generalized matrix $H(q)$ satisfies $h_l I_{m\times m} \le H(q) \le h_u I_{m\times m}$, where h_l, h_u are positive constants.

Property 2. $\dot{H}(q) - 2C(q, \dot{q})$ is a skew symmetric matrix.

Property 3. For $v, v_1, v_2 \in \mathbb{R}^m$ and constant $c_v > 0$, $C(v, v_1)v_2 = C(v, v_2)v_1$ and $|C(v, v_1)| \le c_v|v_1|$.

In contrast to tracking, which involves enforcing control laws to enable the robot to achieve and follow a temporally parameterized path, maneuvering does not require a temporal specification and can be adapted to more flexible work scenarios. Additionally, the challenges posed by sudden actuator failures due to prolonged working hours and unmeasurable speed resulting from cost-saving measures also need to be taken into consideration. The objective of this paper is to develop an output feedback fault-tolerant maneuvering controller with prescribed performance to achieve the following goals:

1) The desired path of the EL system can be described by such a continuous parameterization set

$$\mathcal{S} = \{q_d \in \mathbb{R}^m : \exists\, \varrho \in \mathbb{R} \text{ s.t. } q(t) = q_d(\varrho(t))\},$$

where $\varrho(t)$ is the path variable. The maneuvering task involves the geometric path and dynamic specifications, in this case at the path and velocity aspect, namely

$$\begin{aligned} \lim_{t\to\infty} E\,|q(t) - q_d(\varrho(t))|^2 &\le r_1, \\ \lim_{t\to\infty} E\,|\dot{\varrho}(t) - v_s(\varrho(t), t)|^2 &\le r_2, \end{aligned} \tag{2.2}$$

where $r_1, r_2 > 0$, $v_s(\varrho(t), t)$ is velocity assignment.

2) The path error $\tilde{q} = q(t) - q_d(\varrho(t))$ satisfies the desired prescribed performance

$$-a_2\rho < \tilde{q} < a_1\rho,$$

where $a_1, a_2 > 0$ and ρ is a vector of monotonically decreasing performance function.

3) All signals in a closed-loop system are bounded in probability.

For this end, the following assumptions are introduced for system (2.1).

Assumption 1. There is a constant $\phi > 0$ such that $|\Phi(q)| \leq \phi$.

Assumption 2. The stochastic process $\xi(t)$ is strongly bounded in probability; there exists a constant $M > 0$ such that

$$P(\sup_{t\geq t_0} |\xi(t)|^2 \geq M) \leq \varepsilon, \ \forall \varepsilon > 0.$$

Assumption 3. The path signal $q_d(\varrho)$ and the velocity distribution signal $v_s(\varrho, t)$ are bounded, and the partial derivatives are also bounded.

Remark 1. The distinction between trajectory tracking and maneuverability lies in their respective domains of definition. Trajectory tracking pertains to the temporal domain, requiring a robot to traverse a given trajectory within a specified time frame. Conversely, maneuverability concerns the geometric domain, requiring the robot's trajectory to traverse the actual distance along the reference trajectory. From this, it can be inferred that trajectory tracking is a specific instance of maneuvering.

3. Main results

During the execution of a robotic task, mechanical wear and tear is inevitable due to the uncertainties in the external environment and prolonged operation of the drive mechanisms, which makes these movable mechanical components prone to failure. To effectively address this issue effectively, adaptive projection operators are employed for loss of effectiveness in this section. Additionally, a velocity observer is devised to estimate immeasurable state.

To better handle the partial loss of effectiveness fault matrix δ, a simple transformation is used

$$\delta u = \bar{u}\bar{\delta} \tag{3.1}$$

where $\bar{u} = \text{diag}\{u_1, \cdots, u_m\}, \bar{\delta} = [\delta_1, \cdots, \delta_m]^T$. Based on (3.1) and defining $\dot{q} = v$, the original system (2.1) can be organized in the lower triangle form

$$\begin{aligned} \dot{q} &= v, \\ H(q)\dot{v} &= -C(q, v)v - h(q) - kv + \bar{u}\bar{\delta} + \Phi(q)\xi. \end{aligned} \tag{3.2}$$

3.1. Observer design

In order to deal with the unmeasured velocity, a simpler observer is skillfully designed

$$H(q)\dot{\hat{v}} = -C(q, \hat{v})\hat{v} - h(q) - k\hat{v} + \bar{u}\hat{\bar{\delta}} + K_v H(q)\tilde{v}, \tag{3.3}$$

where $K_v > 0$, $\hat{v}, \hat{\bar{\delta}}$ is the estimations of $v, \bar{\delta}$, the estimation errors are naturally defined as $\tilde{v} = v - \hat{v}$, $\tilde{\bar{\delta}} = \bar{\delta} - \hat{\bar{\delta}}$. From (3.2), (3.3), and Property 3, one obtains

$$H(q)\dot{\tilde{v}} = - C(q, v)\tilde{v} - C(q, \hat{v})\tilde{v} - k\tilde{v} + \bar{u}\tilde{\bar{\delta}} + \Phi(q)\xi - K_v H(q)\tilde{v}. \tag{3.4}$$

Choose the Lyapunov function

$$V_0 = \frac{1}{2}\tilde{v}^T H(q)\tilde{v} + \frac{1}{2}\tilde{\bar{\delta}}^T \mu^{-1}\tilde{\bar{\delta}}, \tag{3.5}$$

where μ^{-1} is a positive definite symmetric constant matrix, and two positive constants μ_l, μ_u can be found such that $0 < \mu_l I_{m\times m} \leq \mu^{-1} \leq \mu_u I_{m\times m}$ holds. Based on (3.4), the derivative of (3.5) is

$$\begin{aligned} \dot{V}_0 =& \tilde{v}^T H(q)\dot{\tilde{v}} + \frac{1}{2}\tilde{v}^T \dot{H}(q)\tilde{v} + \dot{\tilde{\bar{\delta}}}^T \mu^{-1}\tilde{\bar{\delta}} \\ =& \tilde{v}^T(-C(q,\hat{v})\tilde{v} - k\tilde{v} + \bar{u}\tilde{\bar{\delta}} + \Phi(q)\xi - K_v H(q)\tilde{v}) - \dot{\tilde{\bar{\delta}}}^T \mu^{-1}\tilde{\bar{\delta}}, \end{aligned} \tag{3.6}$$

which used Property 2. Inspired by [32], in order to make $\hat{\delta}_i, (i = 1, \cdots, m)$ fall in the interval $[\delta_0, 1]$, the following projection operator is given:

$$\dot{\tilde{\bar{\delta}}} = \mathrm{Proj}_{[\delta_0,1]}\{\mu\bar{u}\tilde{v}\} - o\mu\hat{\bar{\delta}}, \tag{3.7}$$

where $o = \mathrm{diag}\{o_1, \cdots, o_m\}$ with parameter $o_i > 0$, let $\omega = [\omega_1, \cdots, \omega_m]^T = \bar{u}\tilde{v}$, for $i = 1, \cdots, m$, the projection operator is

$$\mathrm{Proj}_{[\delta_0,1]}\{\mu_i\omega_i\} = \begin{cases} \mu_i\omega_i, & \delta_0 < \hat{\delta}_i < 1, \\ \mu_i\omega_i, & \omega_i < 0 \text{ and } \hat{\delta}_i = 1, \\ 0, & \omega_i \geq 0 \text{ and } \hat{\delta}_i = 1, \\ 0, & \omega_i \leq 0 \text{ and } \hat{\delta}_i = \delta_0, \\ \mu_i\omega_i, & \omega_i > 0 \text{ and } \hat{\delta}_i = \delta_0. \end{cases}$$

On the strength of (3.7), the projection operator $\mathrm{Proj}_{[\delta_0,1]}\{\mu w\}$ makes $\tilde{v}^T\bar{u}\tilde{\bar{\delta}} - \tilde{\bar{\delta}}^T\mu^{-1}\dot{\tilde{\bar{\delta}}} \leq -\frac{1}{2}o\tilde{\bar{\delta}}^T\tilde{\bar{\delta}} + \frac{1}{2}o\bar{\delta}^T\bar{\delta}$ hold. By the aid of Young's inequality and Assumption 1, one has

$$\tilde{v}^T\Phi(q)\xi \leq d_1\tilde{v}^T\tilde{v} + \frac{\phi^2}{4d_1}|\xi|^2, \tag{3.8}$$

where $d_1 > 0$. Substituting (3.7) and (3.8) into (3.6), along with Properties 1 and 3, the dynamic of V_0 becomes

$$\begin{aligned} \dot{V}_0 \leq& \tilde{v}^T(-C(q,\hat{v})\tilde{v} + d_1\tilde{v} - k\tilde{v} - K_v H(q)\tilde{v}) + o\tilde{\bar{\delta}}^T\hat{\bar{\delta}} + \frac{\phi^2}{4d_1}|\xi|^2 \\ \leq& -(K_v h_l + \underline{k} - c_{v1}|\hat{v}| - d_1)|\tilde{v}|^2 - \frac{1}{2}o\tilde{\bar{\delta}}^T\tilde{\bar{\delta}} + \frac{1}{2}o\bar{\delta}^T\bar{\delta} + \frac{\phi^2}{4d_1}|\xi|^2, \end{aligned} \tag{3.9}$$

where $c_{v1} > 0$, the minimum eigenvalue of the diagonal matrix k is $\lambda_{\min}(k) = \underline{k}$.

Remark 2. Unlike the globally stable observer design in [29], the speed observer designed in (3.3) exhibits a simplified structure and a clear structure of the system.

3.2. Controller design

For performance-critical applications, it is imperative to not only achieve geometric tasks but also to fulfill both the prescribed transient and steady-state performance requirements. Therefore, the investigation of prescribed performance control for geometric tasks is of considerable significance.

By combining (3.2) and (3.3), the unmeasurable velocity v is replaced by $\hat{v} + \tilde{v}$, then the control system is rewritten as

$$\begin{aligned} \dot{q} &= \hat{v} + \tilde{v}, \\ H(q)\dot{\hat{v}} &= -C(q,\hat{v})\hat{v} - k\hat{v} - h(q) + \hat{\delta}u + K_v H(q)\tilde{v}, \end{aligned} \tag{3.10}$$

where $\hat{\delta} = \text{diag}\{\hat{\delta}_1, \cdots, \hat{\delta}_m\}$. In the following, a prescribed performance control and a dynamic control are designed to accomplish the goals; for (3.10), the associated coordinate transformations are given as

$$\begin{aligned} \tilde{q} &= q - q_d(\varrho), \\ \tilde{v}_d &= \hat{v} - \alpha_d = \hat{v} - \alpha - b, \\ \varpi &= \dot{\varrho} - v_s(\varrho, t), \end{aligned} \tag{3.11}$$

where α is a stabilization function and $b = \alpha_d - \alpha$ is filter error, and ϖ is speed distribution error. To avoid differentiation of α, borrowing the dynamic surface technique from [33], the filter with time constant κ is used; that is,

$$\kappa\dot{\alpha}_d + \alpha_d = \alpha, \ \alpha_d(0) = \alpha(0).$$

Step 1. The predefined performance requirement in vector form is

$$-a_2\rho < \tilde{q} < a_1\rho, \tag{3.12}$$

where $\tilde{q} = [\tilde{q}_1, \cdots, \tilde{q}_m]^T, \rho = [\rho_1, \ldots, \rho_m]^T$, for $i = 1, \cdots, m$, the function $\rho_i = (\rho_{i0} - \rho_{i\infty})e^{-\bar{k}_i t} + \rho_{i\infty}$ with $\bar{k}_i > 0, \rho_{i0} > \rho_{i\infty} > 0$. Inspired by [25], introducing the error transfer function $z = [z_1, \cdots, z_m]^T$ to deal with performance constraint, that is

$$z_i = \frac{a_1\tilde{q}_i}{a_1\rho_i - \tilde{q}_i}h(\tilde{q}_i) + \frac{a_2\tilde{q}_i}{a_2\rho_i + \tilde{q}_i}(1 - h(\tilde{q}_i)), \tag{3.13}$$

where $h(\tilde{q}_i) = 1$, as $\tilde{q}_i \geq 0$, and $h(\tilde{q}_i) = 0$, as $\tilde{q}_i < 0$. According to (3.13), it is straightforward to verify that z_i will tend to infinity when the path error $\tilde{q}_i$ approaches $a_1\rho_i$ or $-a_2\rho_i$. Therefore, if z_i is controlled to be bounded, $\tilde{q}_i$ will satisfy the prescribed error constraint (3.12).

Choose Lyapunov function $V_1 = \frac{1}{2}z^T z$, whose derivative satisfies

$$\begin{aligned} \dot{V}_1 &= z^T(\dot{\tilde{q}}\Lambda\rho - \tilde{q}\Lambda\dot{\rho}) \\ &= z^T((\tilde{v}_d + \alpha + b + \tilde{v} - \frac{\partial q_d}{\partial \varrho}(\varpi + v_s)\Lambda\rho) - \tilde{q}\Lambda\dot{\rho}), \end{aligned}$$

where $\Lambda = [\Lambda_1, \cdots, \Lambda_m] \in \mathbb{R}^{1\times m}$ with $\Lambda_i = \frac{a_1^2}{(a_1\rho_i - \tilde{q}_i)^2}h(\tilde{q}_i) + \frac{a_2^2}{(a_2\rho_i + \tilde{q}_i)^2}(1 - h(\tilde{q}_i))$. Select α as

$$\alpha = \frac{\partial q_d}{\partial \varrho}v_s + \frac{1}{\Lambda\rho}(-c_1 z + \tilde{q}\Lambda\dot{\rho}), \tag{3.14}$$

where $c_1 > 0$. Then the derivative of V_1 turns into

$$\dot{V}_1 = -c_1 z^T z + z^T((\tilde{v}_d + b + \tilde{v} - \frac{\partial q_d}{\partial \varrho}\varpi)\Lambda\rho). \tag{3.15}$$

Step 2. Choose the candidate Lyapunov function as

$$V_2 = V_1 + \frac{1}{2}\tilde{v}_d^T\tilde{v}_d + \frac{1}{2\lambda\gamma}\varpi^2 \tag{3.16}$$

with $\lambda, \gamma > 0$, according to (3.10), (3.11), and (3.15), one has

$$\begin{aligned}\dot{V}_2 =& - c_1|z|^2 + z^T((b + \tilde{v} - \frac{\partial q_d}{\partial \varrho}\varpi)\Lambda\rho) + \tilde{v}_d^T(H^{-1}(q)(-C(q,\hat{v})\hat{v} - k\hat{v} - h(q) + \hat{\delta}u \\ &+ K_v H(q)\tilde{v}) + \Lambda\rho z - \dot{\alpha}_d) + \frac{1}{\lambda\gamma}\varpi\dot{\varpi},\end{aligned}$$

by using Young's inequality, one holds $\tilde{v}_d^T K_v\tilde{v} \leq \frac{1}{4d_2}|\tilde{v}|^2 + d_2K_v^2|\tilde{v}_d|^2$ with $d_2 > 0$. Naturally, choose the control input u as

$$u = \hat{\delta}^{-1}(H(q)(-c_2\tilde{v}_d - d_2K_v^2\tilde{v}_d - \Lambda\rho z + \dot{\alpha}_d) + C(q,\hat{v})\hat{v} + k\hat{v} + h(q)), \tag{3.17}$$

where $c_2 > 0$. Then, the derivative of V_2 becomes

$$\dot{V}_2 = - c_1|z|^2 - c_2|\tilde{v}_d|^2 + z^T((b + \tilde{v} - \frac{\partial q_d}{\partial \varrho}\varpi)\Lambda\rho) + \frac{1}{4d_2}|\tilde{v}|^2 + \frac{1}{\lambda\gamma}\varpi\dot{\varpi}. \tag{3.18}$$

3.3. Stability analysis

In this subsection, an update law is designed to realize dynamic tasks, and Lyapunov proof is given to analyze the stability of the closed-loop system. The whole Lyapunov function is selected as

$$V = V_0 + V_2 + \frac{1}{2}b^Tb, \tag{3.19}$$

where the dynamic equation of filter error satisfies

$$\dot{b} = -\frac{b}{\kappa} - \dot{\alpha}. \tag{3.20}$$

By the aid of (3.9), (3.18) and (3.20), one has

$$\dot{V} = \dot{V}_0 + \dot{V}_2 - b^T(\frac{b}{\kappa} + \dot{\alpha}). \tag{3.21}$$

For state set $\chi = [\tilde{v}^T, \tilde{\tilde{\delta}}^T, z^T, \tilde{v}_d^T, b^T, \varpi]^T$, the Lyapunov function (3.19) can be constructed as

$$a_3|\chi|^2 \leq V(\chi) \leq a_4|\chi|^2, \tag{3.22}$$

where $a_3 = \frac{1}{2}\min\{1, h_l, \mu_l, \frac{1}{\lambda\gamma}\}$, $a_4 = \frac{1}{2}\min\{1, h_u, \mu_u, \frac{1}{\lambda\gamma}\}$. For any constant $v_0 > 0$, denote $r_0 = \sqrt{\frac{v_0}{a_4}}$, consider the ball $B(0, r_0) = \{\chi : |\chi(0)| \leq r_0\}$ as a compact set, where the constants $e_j(j = 1, \cdots, 4)$ can always be found to satisfy the following inequality:

$$|\dot{\alpha}| \leq e_1|z| + e_2|\tilde{v}_d| + e_3|\varpi| + e_4.$$

Employing Young's inequality and Property 1, one obtains

$$\begin{aligned}
\Lambda\rho z^T\tilde{v} &\le d_3(\Lambda\rho)^2|z|^2 + \frac{1}{4d_3}|\tilde{v}|^2,\\
\Lambda\rho z^T b &\le d_4(\Lambda\rho)^2|z|^2 + \frac{1}{4d_4}|b|^2,\\
b^T\dot{\alpha} &\le p_0|b|^2 + \frac{1}{d_5}(|z|^2 + |\tilde{v}_d|^2 + |\varpi|^2 + 1),
\end{aligned} \tag{3.23}$$

where $d_i > 0, (i = 3, 4, 5)$, $p_0 = \frac{d_5}{4}\sum_{j=1}^{4} e_j^2$. Combining (3.21) and (3.23), following [17, 18], the filter-gradient update law is designed as

$$\dot{\varpi} = -\lambda\varpi + \lambda\gamma(\Lambda\rho z^T\frac{\partial q_d}{\partial \varrho}\varpi - \frac{1}{d_5}\varpi). \tag{3.24}$$

With the help of (3.23) and (3.24), (3.21) can be rephrased as

$$\begin{aligned}
\dot{V} \le& -(K_v h_l + \underline{k} - c_{v1}|\hat{v}| - d_1 - \frac{1}{4d_2} - \frac{1}{4d_3} - \frac{1}{d_4})|\tilde{v}|^2 - (c_2 - \frac{1}{d_5})|\tilde{v}_d|^2 - (\frac{1}{\kappa} - p_0)|b|^2 - \frac{1}{\gamma}\varpi^2\\
&-(c_1 - d_3(\Lambda\rho)^2 - d_4(\Lambda\rho)^2 - \frac{1}{d_5})|z|^2 - \frac{1}{2}o\tilde{\bar{\delta}}^T\tilde{\bar{\delta}} + \frac{1}{2}o\bar{\delta}^T\bar{\delta} + \frac{1}{d_5} + \frac{\phi^2}{4d_1}|\xi|^2\\
\le& -cV + p_1|\xi|^2 + p_2,
\end{aligned} \tag{3.25}$$

let $K_v = K_{v1} + K_{v2}$, $c_1 = c_{11} + c_{12}$, $c_2 = c_{21} + c_{22}$, $\frac{1}{\kappa} = \frac{1}{\kappa_1} + \frac{1}{\kappa_2}$, and define $c = 2\min\{\frac{K_{v1}h_l}{h_u}, c_{11}, c_{21}, \frac{o}{\mu_u}, \frac{1}{\kappa_1}, \lambda\}$, $\bar{c} = 2\min\{K_{v2}h_l + \underline{k} - c_{v1}|\hat{v}| - d_1 - \frac{1}{4d_2} - \frac{1}{4d_3} - \frac{1}{d_4}, c_{12} - d_3(\Lambda\rho)^2 - d_4(\Lambda\rho)^2 - \frac{1}{d_5}, c_{22} - \frac{1}{d_5}, \frac{1}{\kappa_2} - p_0\}$, $p_1 = \frac{\phi^2}{4d_1}$, $p_2 = \frac{1}{2}o\bar{\delta}^T\bar{\delta} + \frac{1}{d_5}$. To insure $c > 0, \bar{c} > 0$, the requirements on parameters are

$$\begin{aligned}
&K_{v1} > 0, c_{11} > 0, c_{21} > 0, \kappa_1 > 0, c_{12} > d_3(\Lambda\rho)^2 + d_4(\Lambda\rho)^2 + \frac{1}{d_5},\\
&K_{v2}h_l > c_{v1}|\hat{v}| + d_1 + \frac{1}{4d_2} + \frac{1}{4d_3} + \frac{1}{d_4} - \underline{k}, c_{22} > \frac{1}{d_5}, \frac{1}{\kappa_2} > p_0.
\end{aligned}$$

Ultimately the error system is

$$\begin{aligned}
H(q)\dot{\tilde{v}} =& -C(q,v)\tilde{v} - C(q,\hat{v})\tilde{v} - k\tilde{v} + \bar{u}\tilde{\bar{\delta}} - K_v H(q)\tilde{v} + \Phi(q)\xi,\\
\dot{z} =& -c_1 z - (\tilde{v}_d + \tilde{v} + b - \frac{\partial q_d}{\partial \varrho}\varpi)\Lambda\rho,\\
\dot{\tilde{v}}_d =& -c_2\tilde{v}_d - \Lambda\rho z - d_2K_v^2\tilde{v}_d + K_v\tilde{v},\\
\dot{\varpi} =& -\lambda\varpi + \lambda\gamma(\Lambda\rho z^T\frac{\partial q_d}{\partial \varrho}\varpi - \frac{1}{d_5}\varpi),\\
\dot{\tilde{\bar{\delta}}} =& \text{Proj}_{[\delta_0,1]}\{\mu\omega\} - o\mu\hat{\bar{\delta}}.
\end{aligned} \tag{3.26}$$

To reflect the detailed control process of the random EL system, a technology roadmap shown in Figure 1 is given.

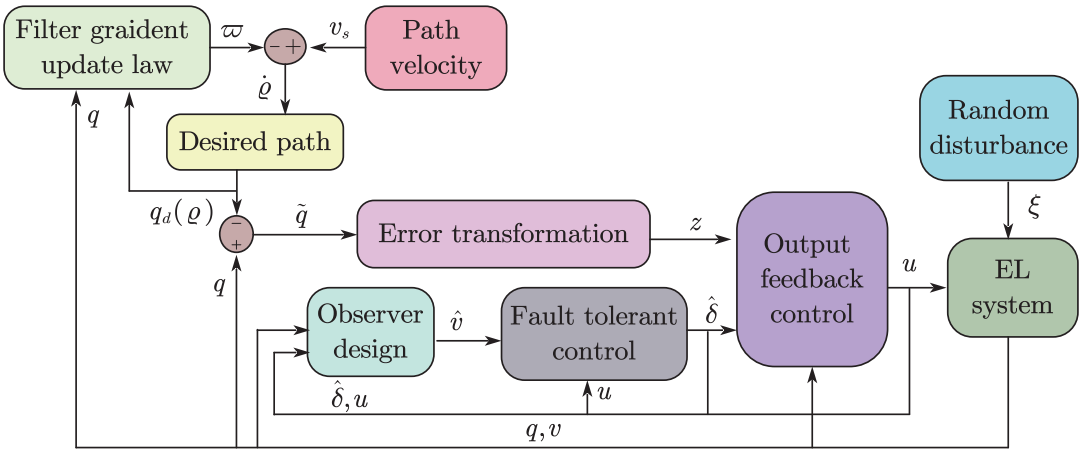

Figure 1. Block diagram of the control of manipulator.

Combining the above analysis, the main results of this section are summarized as the following theorem.

Theorem 1. For the random EL system (2.1) with actuator malfunctions and unmeasurable velocity, under Assumptions 1–3, the observer (3.3) and controllers (3.14), (3.17), (3.24) are designed, then the following properties can be guaranteed:

1) The closed-loop system (3.26) is semi-global noise-to-state practical stability in probability.

2) The maneuvering task is resolved, and the prescribed performance is satisfied.

3) All signals in (3.26) are bounded in probability.

Proof. On the basis of [34], combining (3.22) with (3.25), the closed-loop system is semi-global noise-to-state practical stability in probability; from Gronwall's lemma and Assumption 2, one has

$$E|\chi|^2 \leq \frac{a_4}{a_3}\chi(t_0)^2 e^{-c(t-t_0)} + \frac{p_1 M + p_2}{ca_3}, \tag{3.27}$$

which means

$$\begin{aligned} \lim_{t\to\infty} E|z|^2 &\leq \frac{p_1 M + p_2}{ca_3}, \\ \lim_{t\to\infty} E|\varpi|^2 &\leq \frac{p_1 M + p_2}{ca_3}, \end{aligned} \tag{3.28}$$

owing to the Markov inequality, the maneuvering task in (2.2) holds. If $-a_2\rho(0) < \tilde{q}_d(0) < a_1\rho(0)$, z is bounded, so the error performance constraint (3.12) will not be compromised. The errors can be reduced by adjusting parameters d_1, d_5, o, K_v large enough.

By the aid of (3.27) , the Markov inequality and the definition of χ, the signals $\tilde{v}, \tilde{\bar{\delta}}, \tilde{v}_d$, and ϖ are bounded in probability. Consider the boundedness of reference path signal q_d in Assumption 3, α is bounded, so the control signal u is also bounded in probability. □

Remark 3. Regarding the maneuvering problem of random systems, there is no deterministic equilibrium point in closed-loop systems. In the stability analysis, only practical stability can be achieved, and the practical parameters-tuning principle is adopted for parameter adjustment.

4. Application on random manipulator

A two-link manipulator in random surroundings as a practical example is employed in this subsection. In Figure 2, for the i-th link ($i = 1, 2$), its mass, length, viscous friction, rotation angle, and control force are m_i, l_i, k_i, q_i, and u_i, respectively. $\xi_i, (i = 1, 2, 3)$ represent the disturbance accelerations in three directions.

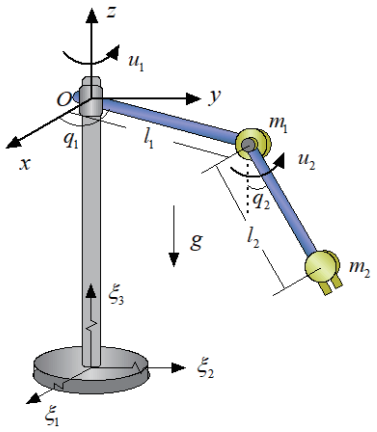

Figure 2. Manipulator in a random vibration workspace.

4.1. Random model

The random model of the manipulator system is

$$H(q)\ddot{q} = -C(q, \dot{q})\dot{q} - h(q) - k\dot{q} + \delta u + \Phi(q)\xi, \tag{4.1}$$

where $q = [q_1, q_2]^T$, $u = [u_1, u_2]^T$, $k = \text{diag}\{k_1, k_2\}$, $\delta = \text{diag}\{\delta_1, \delta_2\}$, $\xi = [\xi_1, \xi_2, \xi_3]^T$, the potential energy vector is $h(q) = [0, m_2 l_2 g \sin q_2]^T$, where g is acceleration of gravity. The inertia matrix is

$$H(q) = \begin{pmatrix} (m_1 + m_2)l_1^2 + m_2 l_2^2 \sin^2 q_2 + 2m_2 l_1 l_2 \sin q_2 & 0 \\ 0 & m_2 l_2^2 \end{pmatrix},$$

the Coriolis matrix is

$$C(q, \dot{q}) = (m_2 l_2^2 \cos q_2 \sin q_2 + m_2 l_1 l_2 \cos q_2) \begin{pmatrix} \dot{q}_2 & \dot{q}_1 \\ -\dot{q}_1 & 0 \end{pmatrix},$$

the random generalized force matrix is

$$\Phi(q) = \begin{pmatrix} -m_1 l_1 \sin q_1 & m_1 l_1 \cos q_1 & 0 \\ m_2 l_2 \cos q_1 \cos q_2 & m_2 l_2 \sin q_1 \cos q_2 & m_2 l_2 \sin q_2 \end{pmatrix}.$$

Drawing on the previous section, an output feedback observer with $m = 2$ is shown in (3.3) with projection operators (3.7), and the static controllers (including virtual controller (3.14) and real controller (3.17)) and dynamic controller (that is, filter-gradient update law (3.24)) corresponding to the dimension are not written repeatedly.

4.2. Simulation

The following simulation results are performed on random manipulator model (4.1). Given the reference signal $q_d(\varrho) = [\cos(0.2\varrho), \sin(0.2\varrho)]^T$ and speed assignment task

$$v_s = \begin{cases} 0.5 \text{ rad/s}, & t \leq 30\text{s}, \\ 1 \text{ rad/s}, & t > 30\text{s}. \end{cases}$$

The path variable ϱ is shown in the first plot of Figure 3; as depicted in the second plot of Figure 3, the dynamic task is effectively realized under the gradient update law.

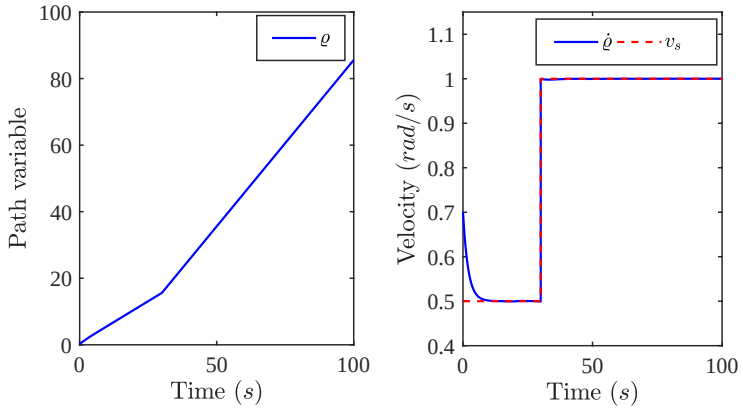

Figure 3. Path variable and speed task.

In simulation, the system parameters are $m_1 = m_2 = 0.01$, $l_1 = 0.4$, $l_2 = 0.5$, $g = 9.8$, $k_1 = 0.4$, $k_2 = 0.2$. The manipulator system is disturbed by colored noise, while the zero-averaged finite bandwidth white noise is linearly filtered to obtain the colored noise, namely, $s_i\dot{\xi}_i(t) = -\xi_i(t) + w_i(t), \xi_i(0) = 0$, for $i = 1, 2, 3$, choose the sample time as $t_c = 0.1$, the constants of noise power are $A_1 = 0.2$, $A_2 = A_3 = 0.1$, the denominator coefficients of the filter as $s_1 = s_2 = 2, s_3 = 1$, and the gains are $b_1 = 1, b_2 = b_3 = 2$. The disturbances in the environment are shown in Figure 4.

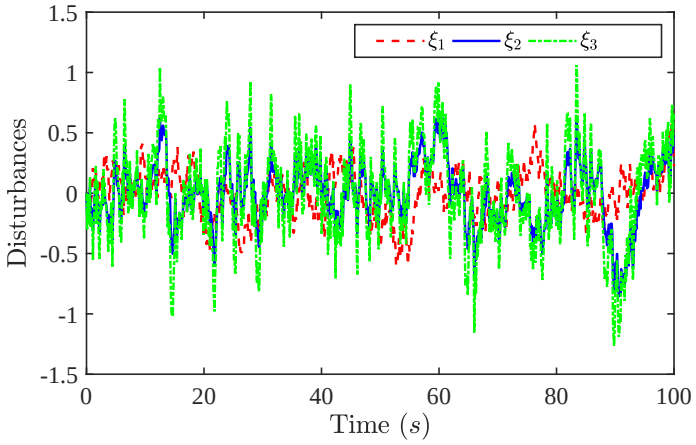

Figure 4. Colored noise.

The initial values are $q(0) = [0.2, 0.1]^T$, $v(0) = [0, 0]^T$, $\hat{v}(0) = [0, 0]^T$, $\alpha_d(0) = [0.1, 0.1]^T$, $\hat{\delta}_1(0) = \hat{\delta}_2(0) = 1$, $\varpi(0) = 0.2$, $\varrho(0) = 0.2$. The control parameters are $c_1 = 0.4, c_2 = 0.6, \mu_1 = 6, \mu_2 = 5, o_1 = 0.0001, o_2 = 0.0002, \lambda = 5, \gamma = 0.02, K_v = 6, d_2 = 0.2, d_5 = 2, \kappa = 0.1, \delta_0 = 0.1$. The parameters of the geometric task constraint performance functions are $a_1 = a_2 = 2, \rho_{10} = \rho_{20} = 1, \rho_{1\infty} = \rho_{2\infty} = 0.1$, $\bar{k}_1 = 0.4, \bar{k}_2 = 0.5$. Due to wear and tear of the devices, the robotic arm system may experience actuator failures, and it is assumed that two controllers will not be inoperative at the same time in order to keep the system running. The actuator loss of effectiveness factors are chosen as

$$\delta_1 = \begin{cases} 1, & t \leq 15\text{s}, \\ 0.5, & t > 15\text{s}, \end{cases} \quad \delta_2 = \begin{cases} 1, & t \leq 20\text{s}, \\ 0.4, & t > 20\text{s}. \end{cases}$$

Under the fault-tolerant control, the simulation results are given in Figure 5, which provides estimated curves of the actuator failure fault factor. At the same time, the performance constraints for the path-following error $z = [z_1, z_2]^T$ are shown in Figure 6.

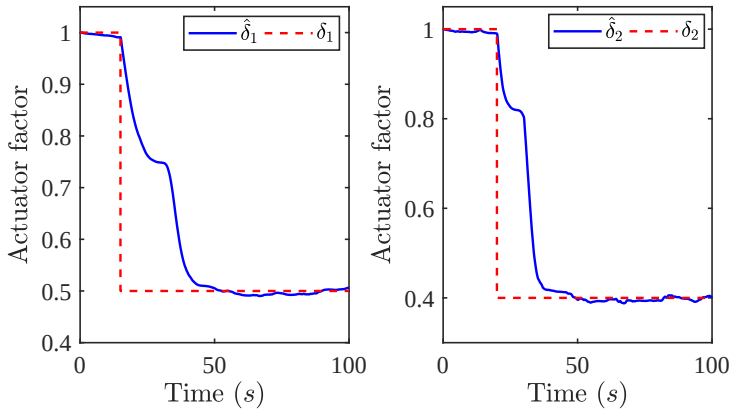

Figure 5. Actuator fault case.

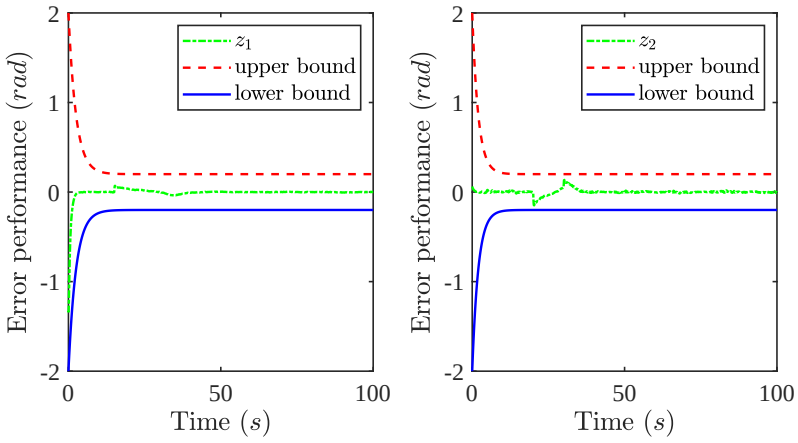

Figure 6. Performance constraint.

As shown in Figure 7, the proposed observer-controller demonstrates effective performance in the maneuvering task while maintaining a sufficiently small observer error. The output signal q can accurately track the reference signal q_d, while the control signal u remains effective under random work surroundings.

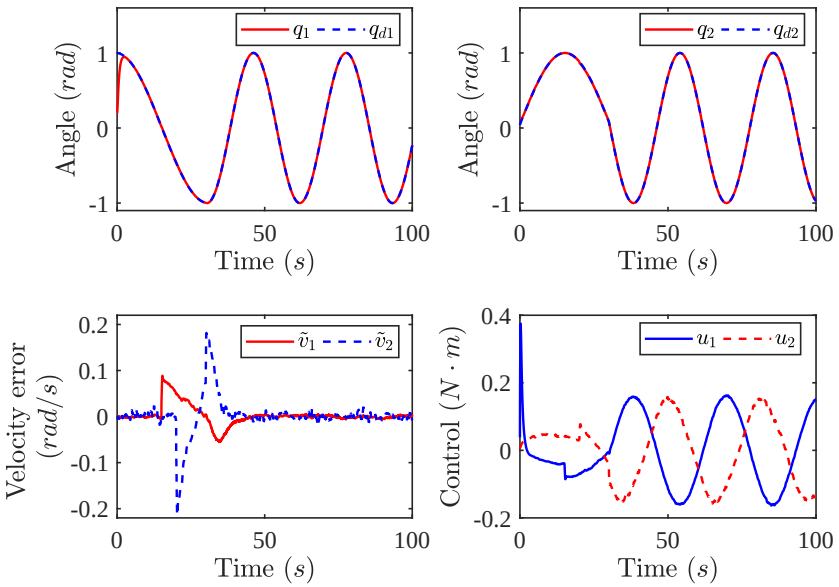

Figure 7. Simulation results.

5. Conclusions

This study proposes an observer-based fault-tolerant control scheme to solve the maneuvering control problem for random Lagrangian systems with immeasurable states and actuator failures. Based on projection operators and velocity observers, a layered approach comprising static control law and filtered gradient update rate is developed to resolve the maneuvering problem. The simulation results comprehensively demonstrate that the designed output feedback maneuvering controller not only guarantees semi-global practical stability of the system but also ensures the boundedness in probability of all signals. Future work will focus on extending these methodologies to address the output feedback maneuvering control problem in underactuated systems while considering broader operational scenarios that incorporate safety constraints.

Use of AI tools declaration

The authors declare they have not used Artificial Intelligence (AI) tools in the creation of this article.

Acknowledgments

This work was supported by the Research Project Initiation Fund (BS202463).

Conflict of interest

The authors declare there are no conflicts of interest.

References

1. Y. M. Zhang, J. Jiang, Bibliographical review on reconfigurable fault-tolerant control systems, *Annu. Rev. Control*, **32** (2008), 229–252. https://doi:10.1016/j.arcontrol.2008.03.008
2. Q. K. Shen, B. Jiang, P. Shi, *Fault Diagnosis and Fault-Tolerant Control Based on Adaptive Control Approach*, Switzerland: Springer, 2017. https://doi.org/10.1007/978-3-319-52530-3
3. S. Barghandan, M. A. Badamchizadeh, M. R. Jahed-Motlagh, Improved adaptive fuzzy sliding mode controller for robust fault tolerant of a quadrotor, *Int. J. Control Autom. Syst.*, **15** (2017), 427–441. http://dx.doi.org/10.1007/s12555-015-0313-7
4. B. Huang, S. Zhang, Y. S. He, B. Wang, Z. C. Deng, Finite-time anti-saturation control for Euler–Lagrange systems with actuator failures, *ISA Trans.*, **124** (2020), 468–477. https://doi.org/10.1016/j.isatra.2020.08.028
5. K. Yan, M. Chen, Q. X. Wu, Neural network-based adaptive fault tolerant tracking control for unmanned autonomous helicopters with prescribed performance, *Proc. Inst. Mech. Eng., Part G: J. Aerosp. Eng.*, **233** (2019), 4350–4362. https://doi.org/10.1177/0954410018823364
6. K. X. Guo, S. K. Lyu, X. Yu, J. Z. Qiao, L. Guo, Y. M. Zhang, Fault-tolerant control design for a class of nonlinear systems with actuator malfunctions, *Int. J. Robust Nonlinear Control*, **32** (2022), 2828–2844. https://doi.org/10.1002/rnc.5752
7. G. Heredia, A. Ollero, Detection of sensor faults in small helicopter UAVs using observer/kalman filter identification, *Math. Probl. Eng.*, **2011** (2011), 174618. https://doi.org/10.1155/2011/174618
8. M. S. Qian, B. Jiang, D. Z. Xu, Fault tolerant tracking control schem for UAV using dynamic surface control technique, *Circ. Syst. Signal Process.*, **31** (2012), 1713–1729. https://doi.org/10.1007/s00034-012-9402-5
9. J. X. Zhang, G. H. Yang, Robust adaptive fault-tolerant control for a class of unknown nonlinear systems, *IEEE Trans. Ind. Electron.*, **64** (2017), 585–594. https://doi.org/10.1109/TIE.2016.2595481
10. Y. X. Li, Finite time command filtered adaptive fault tolerant control for a class of uncertain nonlinear systems, *Automatica*, **106** (2019), 117–123. https://doi.org/10.1016/j.automatica.2019.04.022
11. Y. Liu, X. Q. Yao, W. Zhao, Distributed neural-based fault-tolerant control of multiple flexible manipulators with input saturations, *Automatica*, **156** (2023), 111202. https://doi.org/10.1016/j.automatica.2023.111202
12. J. X. Zhang, G. H. Yang, Fault-tolerant output-constrained control of unknown Euler-Lagrange systems with prescribed tracking accuracy, *Automatica*, **111** (2020), 108606. https://doi.org/10.1016/j.automatica.2019.108606
13. R. Ortega, A. Loria, R. Kelly, A semiglobally stable output feedback PID regulator for robot manipulators, *IEEE Trans. Autom. Control*, **40** (1995), 1432–1436. https://doi.org/10.1109/9.402235
14. S. Islam, P. X. Liu, Output feedback sliding mode control for robot manipulators, *Robotica*, **28** (2010), 975–987. https://doi.org/10.1017/S0263574709990816

15. Ø. N. Stamnes, O. M. Aamo, G. O. Kaasa, A constructive speed observer design for general Euler-Lagrange systems, *Automatica*, **47** (2011), 2233–2238. https://doi.org/10.1016/j.automatica.2011.08.006

16. M. Y. Cui, Z. J. Wu, X. J. Xie, Output feedback tracking control of stochastic Lagrangian systems and its application, *Automatica*, **50** (2014), 1424–1433. http://dx.doi.org/10.1016/j.automatica.2014.03.001

17. R. Skjetne, T. I. Fossen, P. V. Kokotović, Robust output maneuvering for a class of nonlinear systems, *Automatica*, **40** (2004), 373–383. https://doi.org/10.1016/j.automatica.2003.10.010

18. R. Skjetne, T. I. Fossen, P. V. Kokotović, Adaptive maneuvering, with experiments, for a model ship in a marine control laboratory, *Automatica*, **41** (2005), 289–298. https://doi.org/10.1016/j.automatica.2004.10.006

19. Z. H. Peng, D. Wang, T. S. Li, M. Han, Output-feedback cooperative formation maneuvering of autonomous surface vehicles with connectivity preservation and collision avoidance, *IEEE Trans. Syst. Man Cybern.*, **50** (2019), 2527–2535. https://doi.org/10.1109/TCYB.2019.2914717

20. Z. W. Zheng, Moving path following control for a surface vessel with error constraint, *Automatica*, **118** (2020), 109040. https://doi.org/10.1016/j.automatica.2020.109040

21. S. L. Zhao, X. K. Wang, H. Chen, Y. J. Wang, Cooperative path following control of fixed-wing unmanned aerial vehicles with collision avoidance, *J. Intell. Robot. Syst.*, **100** (2020), 1569–1581. https://doi.org/10.1007/s10846-020-01210-3

22. S. Z. Wu, X. Liang, Y. C. Fang, W. He, Geometric maneuvering for underactuated VTOL vehicles, *IEEE Trans. Autom. Control*, **69** (2024), 1507–1519. https://doi.org/10.1109/TAC.2023.3324268

23. Q. L. Hu, X. D. Shao, L. Guo, Adaptive fault-tolerant attitude tracking control of spacecraft with prescribed performance, *IEEE/ASME Trans. Mechatron.*, **23** (2018), 331–341. https://doi.org/10.1109/TMECH.2017.2775626

24. J. Li, J. Y. Li, Z. J. Wu, Y. G. Liu, Practical tracking control with prescribed transient performance for Euler-Lagrange equation, *J. Franklin Inst.*, **357** (2020), 5809–5830. https://doi.org/10.1016/j.jfranklin.2020.03.017

25. C. C. Wang, G. H. Yang, Observer-based adaptive prescribed performance tracking control for nonlinear systems with unknown control direction and input saturation, *Neurocomputing*, **284** (2018), 17–26. https://doi.org/10.1016/j.neucom.2018.01.023

26. X. D. Shao, Q. L. Hu, Y. Shi, B. Y. Jiang, Fault-tolerant prescribed performance attitude tracking control for spacecraft under input saturation, *IEEE Trans. Control Syst. Technol.*, **28** (2018), 574–582. https://doi.org/10.1109/TCST.2018.2875426

27. Z. W. Zheng, M. Feroskhan, Path following of a surface vessel with prescribed performance in the presence of input saturation and external disturbances, *IEEE/ASME Trans. Mechatron.*, **22** (2017), 2564–2575. https://doi.org/10.1109/TMECH.2017.2756110

28. R. P. Xi, H. G. Zhang, Y. F. Mu, J. Zhang, Command filtered tracking control for random nonlinear systems with actuator faults, *IEEE Trans. Circuits Syst. II Express Briefs*, **70** (2022), 221–225. https://doi.org/10.1109/TCSII.2022.3195934

29. M. Y. Cui, C. Yang, Z. J. Wu, Global trajectory tracking of a class of manipulators without velocity measurements in random surroundings, *Int. J. Control*, **95** (2022), 3127–3136. https://doi.org/10.1080/00207179.2021.1957154

30. X. H. Yu, T. Wang, J. B. Qiu, H. J. Gao, Barrier lyapunov function-based adaptive fault-tolerant control for a class of strict-feedback stochastic nonlinear systems. *IEEE Trans. Cybern.*, **51** (2019), 938–946. https://doi.org/10.1109/TCYB.2019.2941367

31. W. Sun, S. F. Su, J. W. Xia, G. M. Zhuang, Command filter-based adaptive prescribed performance tracking control for stochastic uncertain nonlinear systems, *IEEE Trans. Syst. Man Cybern. Syst.*, **50** (2020), 6555–6563. https://doi.org/10.1109/TSMC.2019.2963220

32. K. Yan, M. Chen, B. Jiang, Q. X. Wu, Robust adaptive active fault-tolerant control of uah with unknown disturbances and actuator faults, *Int. J. Adapt. Control Signal Process.*, **33** (2019), 684–711. https://doi.org/10.1002/acs.2979

33. D. Swaroop, J. K. Hedrick, P. P. Yip, J. C. Gerdes, Dynamic surface control for a class of nonlinear systems, *IEEE Trans. Autom. Control*, **45** (2000), 1893–1899. https://doi.org/10.1109/TAC.2000.880994

34. C. Yang, Z. J. Wu, L. K. Feng, Semi-global practical stability of random systems and its application, *J. Syst. Sci. Complexity*, **36** (2023), 2398–2414. https://doi.org/10.1007/s11424-023-2463-7

AIMS Press